Intersubband electroluminescence from Si/SiGe cascade emitters at terahertz frequencies

S. A. Lynch, R. Bates, D. J. Paul, D. J. Norris, A. G. Cullis, Z. Ikonic, R. W. Kelsall, P. Harrison, D. D. Arnone, and C. R. Pidgeon

Citation: Applied Physics Letters **81**, 1543 (2002); doi: 10.1063/1.1501759
View online: http://dx.doi.org/10.1063/1.1501759
View Table of Contents: http://scitation.aip.org/content/aip/journal/apl/81/9?ver=pdfcov
Published by the AIP Publishing

Intersubband electroluminescence from Si/SiGe cascade emitters at terahertz frequencies

S. A. Lynch, R. Bates, and D. J. Paul[a)]
Cavendish Laboratory, University of Cambridge, Madingley Road, Cambridge, CB3 0HE, United Kingdom

D. J. Norris and A. G. Cullis
Department of Electronic and Electrical Engineering, University of Sheffield, Mappin Street, Sheffield, S1 3JD, United Kingdom

Z. Ikonic, R. W. Kelsall, and P. Harrison
Institute for Microwaves and Photonics, School of Electronic and Electrical Engineering, University of Leeds, Leeds, LS2 9JT, United Kingdom

D. D. Arnone
TeraView Ltd., 302-304 Science Park, Milton Road, Cambridge, CB4 4WE, United Kingdom

C. R. Pidgeon
Department of Physics, Heriot-Watt University, Riccarton, Edinburgh, EH14 4AS, United Kingdom

(Received 27 December 2001; accepted for publication 26 June 2002)

The quantum cascade laser provides one possible method of realizing high efficiency light emitters in indirect band gap materials such as silicon. Electroluminescence results from Si/SiGe quantum cascade emitters are presented demonstrating edge emission from heavy-hole to heavy-hole transitions and light-hole to heavy-hole transitions. In surface-normal emission, only light-hole to heavy-hole electroluminescence is observed as predicted by theory. Intersubband emission is demonstrated at 2.9 THz (103 μm wavelength), 8.9 THz (33.7 μm), and 16.2 THz (18.5 μm) from the Si/SiGe quantum cascade heterostructures. © *2002 American Institute of Physics.*
[DOI: 10.1063/1.1501759]

At present, the terahertz region of the electromagnetic spectrum (1 to 10 THz) is underutilized due to an absence of practical sources and detectors. There are, however, a number of potential applications including medical imaging[1] (including dental[1] and skin cancer),[2] biological weapon detection, security monitoring, gas sensing,[3] pollution monitoring, and molecular spectroscopy.[4] No practical materials exist with appropriate band gaps to allow interband light-emitting diodes or lasers at the appropriate terahertz frequencies. Intersubband transitions, however, potentially allow photon emission energies in the terahertz region of the spectrum by using band gap engineering. Such structures in the form of the quantum cascade laser[5,6] are already well established in III–V materials at midinfrared frequencies.

While a III–V terahertz quantum cascade laser is certainly feasible[7,8] a silicon-based laser would have considerable advantages. One significant advantage is the absence of strong polar optical phonon scattering in group IV semiconductors which potentially should allow high-temperature operation.[9] Intersubband lifetime measurements of GaAs quantum wells has demonstrated the dominance of polar optical phonon scattering above $\sim$40 K in reducing the nonradiative intersubband lifetimes.[10,11] Similar studies on Si/SiGe heterostructures have demonstrated no reduction in lifetimes up to 100 K.[12,13] Other advantages include low cost, mature silicon processing techniques, and the ability to integrate silicon-based optoelectronics with silicon microelectronics. Midinfrared Si/SiGe cascade emitters have been demonstrated using heavy-hole (HH) to HH intersubband transitions.[14] Previously, light hole (LH) to HH intersubband electroluminescence has been demonstrated by applying electric fields along modulation-doped p-type Si/SiGe heterostructures.[15] This letter demonstrates far-infrared (THz) electroluminescence from Si/SiGe quantum cascade heterostructures.

The wafers for the work were purchased from QinetiQ (formerly DERA, Malvern), U.K. and were grown in an Applied Centura low-pressure chemical vapor deposition growth system on 150 mm p^- Si (100) wafers. SiH_4 and GeH_4 were used in a H_2 carrier gas and B_2H_6 was used for p-type doping. Details of typical growth parameters may be found in references Refs. 16 and 17. The active layers were strain symmetrized on top of strain relaxed $Si_{0.77}Ge_{0.23}$ buffers which involved the growth of a 3 μm thick linearly graded $Si_{1-x}Ge_x$ buffer followed by 1 μm of relaxed $Si_{0.77}Ge_{0.23}$.[16,17] Three separate wafers have been grown and studied but only the results of one will be presented for brevity. The wafer consisted of 400 nm p-$Si_{0.77}Ge_{0.23}$ ($N_A = 1 \times 10^{19}$ cm^{-3} B), a 30 nm graded injector (collector) layer from i-$Si_{0.77}Ge_{0.23}$ to i-$Si_{0.72}Ge_{0.28}$, then thirty periods of 5 nm i-Si barriers with 8 nm i-$Si_{0.72}Ge_{0.28}$ quantum wells (Fig. 1). The cascade was capped with a 30 nm graded injector (collector) and 80 nm p-$Si_{0.77}Ge_{0.23}$ contact layer. The layer thicknesses have been measured by transmission electron microscopy (TEM), the Ge fractions by energy dispersive x-ray spectroscopy (EDX) along with energy filtered TEM and the doping densities by secondary ion mass spectrometry (SIMS).

a)Electronic mail: dp109@cam.ac.uk

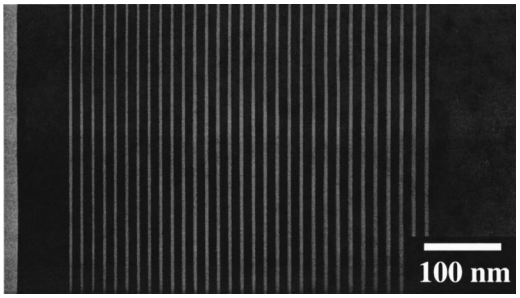

FIG. 1. A transmission electron micrograph of the 30 period quantum wells and barriers at the surface of the wafer.

Samples were etched into $180\times180\ \mu m^2$ mesas using CHF_3 and H_2 reactive ion etching[18] and ohmic contacts were made by sintering evaporated Al (1% Si). The contact geometry is shown in the inset of Fig. 2. Figure 2 also shows (solid line) the typical current–voltage characteristic for this device. The curve exhibits evidence of non-linearities in the 1 to 2 V region. This is highlighted by taking the derivative of the current with respect to the voltage (dotted line). The existence of this nonlinearity provides strong evidence that some carriers are quantum mechanically tunneling through the device. Figure 3 shows a logarithmic plot of the emitted power with current for three heatsink temperatures. For this measurement, the device was biased with a pulsed current source with 50% duty cycle. The graph of Fig. 3 highlights two different regimes of operation. Above 7 mA, the power scales as the square of the bias current. This type of behavior is consistent with Joule heating of the device at high currents. In contrast, below 7 mA, the emitted power scales quite linearly with current. This graph provides strong evidence that the emission is predominately intersubband at low bias currents.

Fourier transform infrared spectroscopy was performed using a Bruker 66V stepscan spectrometer with a liquid-He cooled Si bolometer for detection. The sample was placed in a continuous flow cryostat allowing measurement temperatures between 4.2 and 300 K. A pulsed voltage was applied to the sample at 413 Hz with a variable duty cycle and the bolometer signal was measured using a lock-in amplifier with the pulsed voltage signal as reference. The bias voltage was applied vertically across the 30 quantum wells in the sample. All parts of the system in which THz radiation propagates were kept in a vacuum to eliminate absorption from air or water vapor. Four different samples have been measured from the present wafer all demonstrating nominally identical properties. The devices exhibited electroluminescence over a significant temperature range though the signal became weaker as the heatsink temperature was increased. Figure 4 shows a surface-normal emission spectrum recorded at 2 V at a heatsink temperature of 40 K (solid line). The spectrum shows a well defined peak at 2.9 THz. The dotted line shows the calculated spectrum obtained using a six-band $\mathbf{k}\cdot\mathbf{p}$ model with self-consistent inclusion of the internal charge density using the widths and Ge contents of the quantum wells obtained from TEM and EDX. The graph shows excellent agreement between experiment and calculation, in both spectral position and width. Selection rules dictate that only the HH1–LH1 may be observed in surface emission.

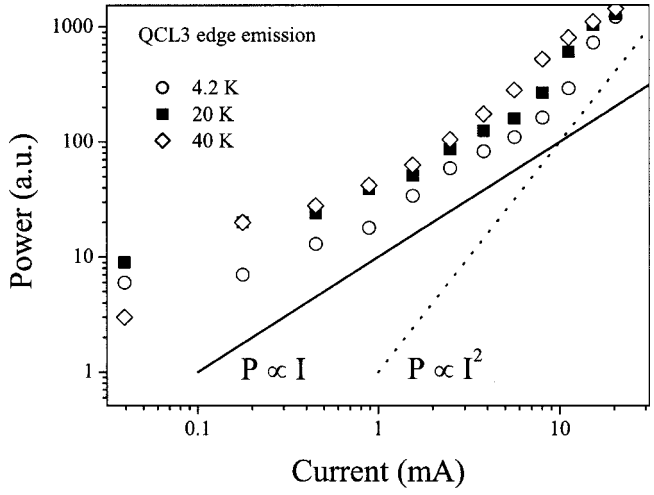

FIG. 3. Logarithmic plot of the emitted power versus current for three temperatures. The duty cycle was 50%. The solid and dotted lines illustrate ideal linear and quadratic power dependencies, respectively.

Figure 5 shows the electroluminescence spectrum collected from the edge of the device. Here, the voltage was

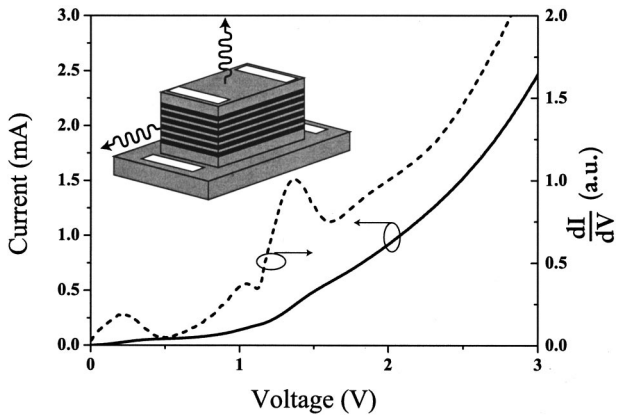

FIG. 2. Current–voltage characteristics (solid line) and the derivative of the current with respect to voltage (dotted line). Inset shows the device geometry.

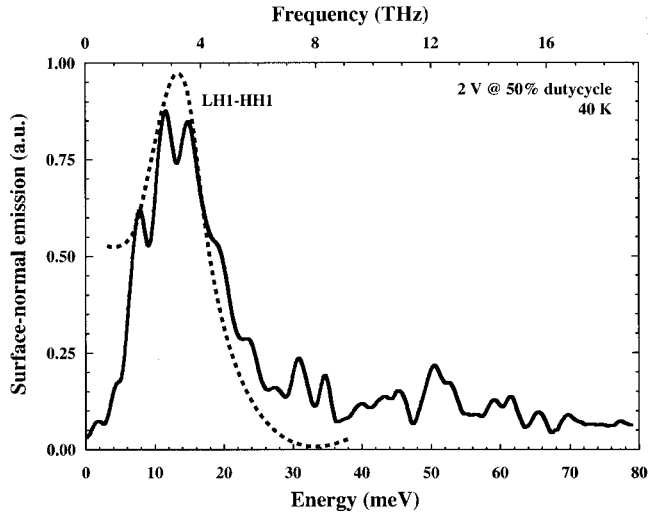

FIG. 4. The measured surface-normal electroluminescence for the cascade wafer (solid line) at 40 K and 2 V applied voltage for a 50% duty cycle. The theoretically calculated spectrum for the LH1–HH1 transition is also shown (dotted line).

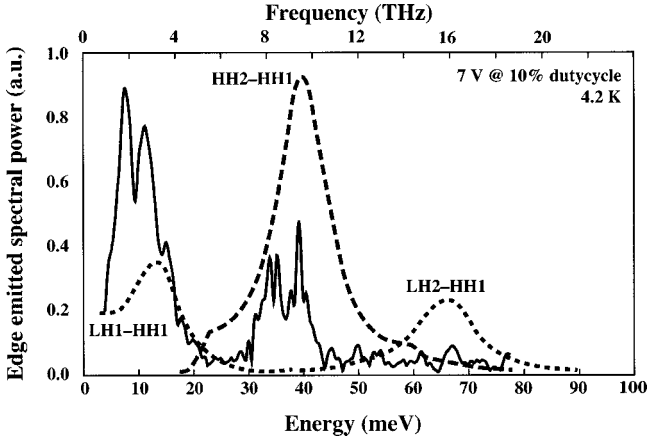

FIG. 5. The experimental edge-emission electroluminescence spectrum for an applied bias voltage of 7 V at 4.2 K (solid line) for a 10% duty cycle. Also the calculated edge-emission spectrum for the cascade wafer (dotted lines) showing the LH1–HH1, HH2–HH1, and LH2–HH1 transitions.

increased to 7 V and the duty cycle was correspondingly reduced to 10% in order to minimize heating. This spectrum shows an additional strong peak at 8.9 THz. This agrees very well with the calculated HH2–HH1 transition (dotted line). Selection rules dictate that this transition may only be observed in edge emission. A third peak at 16.2 THz close to the noise limit was observed in all measured spectra and is close to the center of the calculated LH2–HH1 transition.

At present, enhanced electroluminescence which is expected from the accurate alignment of the subbands in adjacent quantum wells across the entire cascade structure has not been observed. While current–voltage characteristics suggest that there is tunneling through subbands in adjacent quantum wells, the present emission mechanism especially for the larger applied voltages is predominantly by energetic carriers scattered to bound states within the quantum wells. This allows all bound transitions to be accessed in the edge-emission spectrum at large applied voltages, thereby producing a map of the positions of the lowest subband states in the quantum wells. These subband positions demonstrate excellent agreement with those calculated from the $\mathbf{k}\cdot\mathbf{p}$-theoretical modeling assuming equal populations of the upper subband in each transition. Hence, the theory predicts the HH2 to HH1 transition to be the strongest due to having the largest matrix element, while experimentally the lower energy subbands have higher populations in the upper subband and, hence, are stronger in the experimental data. Intersubband electroluminescence persisted above 77 K (an accurate determination of the highest temperature of emission has not been completed) and the maximum power emitted was measured as 10 nW at 40 K. The power from the Si bolometer was calibrated by using a molecular gas laser with a far-infrared pyroelectric detector.[19]

In conclusion, intersubband electroluminescence from Si/SiGe quantum cascade emitters has been demonstrated at far-infrared (THz) frequencies. Both LH to HH and HH to HH intersubband transitions have been clearly observed. Theoretical calculations have been used to identify the intersubband transitions observed at 2.9 THz (103 μm wavelength), 8.9 THz (33.7 μm), and 16.2 THz (18.5 μm) using structural characterization data from TEM, EDX, and SIMS. The present results suggest that appropriately designed and optimized Si/SiGe heterostructures should allow the realization of a terahertz quantum cascade laser.

This work was funded by U. S. DARPA under Air Force Contract No. F-19628-99-C-0074. The authors would like to thank David Robbins, Richard Soref, and Edgar Martinez for useful discussions and support.

[1] D. D. Arnone, C. M. Ciesla, and M. Pepper, Phys. World **13**, 35 (2000).
[2] R. M. Woodward, B. E. Cole, V. P. Wallace, D. D. Arnone, R. Pye, E. H. Linfield, M. Pepper, and A. G. Davies, *Proceedings of the CLEO* (IEEE, New York, 2001), paper CWE4.
[3] D. M. Mittleman, R. H. Jacobsen, R. Neelamani, R. G. Baraniuk, and M. C. Nuss, Appl. Phys. B: Lasers Opt. **67**, 379 (1998).
[4] F. N. Keutsch, M. G. Brown, P. B. Petersen, R. J. Saykally, M. Geleijns, and A. van der Avoird, J. Chem. Phys. **114**, 3994 (2001).
[5] J. Faist, F. Capasso, D. L. Sivco, C. Sirtori, A. L. Hutchinson, and A. Y. Cho, Science **264**, 553 (1994).
[6] F. Capasso, C. Gmachl, D. L. Sivco, and A. Y. Cho, Phys. World **12**, 27 (1999).
[7] M. Rochat, J. Faist, M. Beck, U. Oesterle, and M. Ilegems, Appl. Phys. Lett. **73**, 3724 (1998).
[8] S. Blaser, M. Rochat, M. Beck, J. Faist, and U. Oesterle, Phys. Rev. B **61**, 8369 (2000).
[9] L. Friedman, G. Sun, and R. A. Soref, Appl. Phys. Lett. **78**, 401 (2001).
[10] B. N. Murdin, W. Heiss, C. J. G. M. Langerak, S. C. Lee, I. Galbraith, G. Strasser, E. Gornik, M. Helm, and C. R. Pidgeon, Phys. Rev. B **55**, 5171 (1997).
[11] C. D. Bezant, M. M. Chamberlain, H. P. M. Pellemans, B. N. Murdin, W. Batty, and M. Henini, Semicond. Sci. Technol. **14**, L25 (1999).
[12] C. R. Pidgeon, P. Murzyn, J-P. R. Wells, I. V. Bradley, Z. Ikonic, R. W. Kelsall, P. Harrison, S. A. Lynch, D. J. Paul, D. D. Arnone, D. J. Robbins, D. J. Norris, and A. G. Cullis, Physica E **13**, 904 (2002).
[13] C. R. Pidgeon, P. Murzyn, J-P. R. Wells, I. V. Bradley, Z. Ikonic, R. W. Kelsall, P. Harrison, S. A. Lynch, D. J. Paul, D. D. Arnone, D. J. Robbins, D. J. Norris, and A. G. Cullis, Appl. Phys. Lett. **80**, 1456 (2002).
[14] G. Dehlinger, L. Diehl, U. Gennser, H. Sigg, J. Faist, K. Ensslin, D. Grützmacher, and E. Müller, Science **290**, 2277 (2000).
[15] S. A. Lynch, S. S. Dhillon, R. Bates, D. J. Paul, D. D. Arnone, D. J. Robbins, Z. Ikonic, R. W. Kelsall, P. Harrison, D. J. Norris, A. G. Cullis, C. R. Pidgeon, P. Murzyn, and A. Loudon, J. Mater. Sci. B **89**, 12 (2002).
[16] D. J. Paul, A. Ahmed, N. Griffin, M. Pepper, A. C. Churchill, D. J. Robbins, and D. J. Wallis, Thin Solid Films **321**, 181 (1998).
[17] A. C. Churchill, D. J. Robbins, D. J. Wallis, N. Griffin, D. J. Paul, A. J. Pidduck, W. Y. Leong, and G. M. Williams, J. Vac. Sci. Technol. B **16**, 1634 (1998).
[18] D. J. Paul, V. J. Law, and G. A. C. Jones, J. Vac. Sci. Technol. B **13**, 2234 (1995).
[19] R. McLaughlin, Q. Chen, A. Corchia, C. M. Ciesla, M. B. Johnson, D. D. Arnone, X.-C. Zhang, G. A. C. Jones, E. H. Linfield, A. G. Davies, and M. Pepper, Appl. Phys. Lett. **76**, 2038 (2000).